2

Lower-and higher-order nonclassical properties of photon added and subtracted displaced Fock state

In this chapter, which is based on Malpani et al. [2019a], we aim to study the nonclassical properties of the PADFS and PSDFS (which are already introduced in Section 1.3.2) using the witnesses of nonclassicality introduced in Section 1.5.1.

2.1 Introduction

As we have mentioned in Chapter 1, with the advent of quantum state engineering Vogel et al. [1993]; Sperling et al. [2014]; Miranowicz and Leonski [2004]; Marchiolli and José [2004] and quantum information processing (Pathak [2013] and references therein), the study of nonclassical properties of engineered quantum states have become a very important field. Quantum state engineering is helpful in realizing non-Gaussianity inducing operations, like photon addition and subtraction Zavatta et al. [2004]; Podoshvedov [2014]. Keeping this in mind, in what follows, in this chapter, we aim to study the nonclassical properties of a set of engineered quantum states (both photon added and subtracted) which can be produced by using the above mentioned techniques.

It is already mentioned in Chapter 1 that a state having a negative P-function is referred to as a nonclassical state. Such a state cannot be expressed as a mixture of coherent states and does not possess a classical analogue. In contrast to these states, coherent states are classical, but neither their finite dimensional versions Miranowicz and Leonski [2004]; Alam et al. [2017c] nor their generalized versions are classical Satyanarayana [1985]; Thapliyal et al. [2016, 2015]; Banerjee and Srikanth [2007]. Here, we would like to focus on photon added and subtracted versions of a particular type of generalized coherent state, which is also referred to as the displaced Fock state (DFS). To be precise, state of the form $|\psi\rangle = D(\alpha)|n\rangle$, where $D(\alpha)$ is the displacement operator with Fock state $|n\rangle$, is referred to as generalized coherent state (see Section 1.3 of Chapter 1), as this state is reduced to a coherent state in the limit $n = 0$. However, from the structure of the state it seems more appropriate to call this state as the DFS, and this seems to be the nomenclature usually adopted

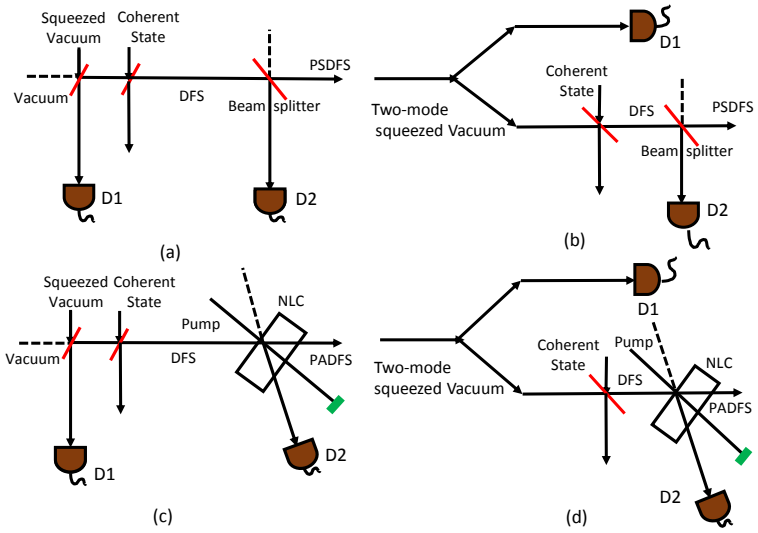

Figure 2.1: A schematic diagram for the generation of PSDFS (in (a) and (b)) and PADFS (in (c) and (d)). In (a) and (c) ((b) and (d)), single-mode (two-mode) squeezed vacuum is used for generation of the desired state. Here, NLC corresponds to nonlinear crystal and D1 and D2 are photon number resolving detectors.

in the literature Keil et al. [2011]; Wunsche [1991]; Blažek [1994]; Moya-Cessa [1995]. In some other works, it is referred to as displaced number state Ziesel et al. [2013]; De Oliveira et al. [2006]; Dodonov and De Souza [2005], but all these names are equivalent; and in what follows, we will refer to it as DFS. This is an extremely interesting quantum state for various reasons. Specifically, its relevance in various areas of quantum optics is known. For example, in the context of cavity QED, it constitutes the eigenstates of the Jaynes-Cummings systems with coherently driven atoms Alsing et al. [1992]. Naturally, various lower-order nonclassical properties and a set of other quantum features of DFS have already been studied. Specifically, quasiprobability distributions of DFS were studied in Wunsche [1991], phase fluctuations of DFS was investigated in Zheng-Feng [1992], decoherence of superposition of DFS was discussed in Dodonov and De Souza [2005], Q function, Wigner function and probability distribution of DFS were studied in De Oliveira et al. [1990], Pancharatnam phase of DFS has been studied in Mendas and Popovic [1993]. Further, in the context of non-optical DFS, various possibilities of generating DFS from Fock states by using a general driven time-dependent oscillator has been discussed in Lo [1991]; and in the trapped-ion system, quantum interference effects have been studied for the superposition of DFS Marchiolli and José [2004]. Thus, DFS seems to be a well studied quantum state, but it may be noted that a little effort has yet been made to study higher-order nonclassical properties of DFS. It is a relevant observation as in the recent past, it has been observed that higher-order nonclassicality has various applications Hillery et al. [1999]; Banerjee et al. [2018]; Sharma et al. [2017]; Thapliyal et al. [2017c], and it can be used to detect the existence of weak nonclassical characters Thapliyal et al. [2014a,b]; Verma and Pathak [2010]; Thapliyal et al. [2017b]; Alam and Mandal [2016a]; Alam et al. [2015]; Thapliyal et al. [2017a]; Prakash and Mishra [2006]; Prakash et al. [2010]; Das et al. [2018]. Further, various higher-order nonclassical features have been experimentally detected Allevi et al. [2012b,a]; Avenhaus et al. [2010]; Peřina Jr et al. [2017]. However, we do not want to restrict to DFS, rather we wish to focus on lower- and higher-order nonclassical properties of a set of even more general states, namely photon added DFS (PADFS) and photon subtracted DFS (PSDFS). The general nature

of these states can be visualized easily, as in the special case that no photon is added (subtracted) PADFS (PSDFS) would reduce to DFS. Further, for $n = 0$, PADFS would reduce to photon added coherent state which has been widely studied (Agarwal and Tara [1991]; Verma et al. [2008]; Thapliyal et al. [2017b] and references therein) and experimentally realized Zavatta et al. [2004, 2005]. Here it is worth noting that DFS has also been generated experimentally by superposing a Fock state with a coherent state on a beam splitter Lvovsky and Babichev [2002]. Further, an alternative method for the generation of DFS has been proposed by Oliveira et al., de Oliveira et al. [2005]. From the fact that photon added coherent state and DFS have already been generated experimentally, and the fact that the photon added states can be prepared via conditional measurement on a beam splitter, it appears that PADFS and PSDFS can also be built in the lab. In fact, inspired by these experiments, we have proposed a schematic diagram for generating the PADFS and PSDFS in Figure 2.1 using single-mode and two-mode squeezed vacuum states. Specifically, using three (two) highly transmitting beam splitters, a conditional measurement of single photons at both detectors D1 and D2 in Figure 2.1 (a) (Figure 2.1 (b)) would result in single photon subtracted DFS as output from a single-mode (two-mode) squeezed vacuum state. Similarly, to generate PADFS conditional subtraction of photon is replaced by photon addition, using a nonlinear crystal and heralding one output mode for a successful measurement of a single photon to ensure generation of single photon added DFS. This fact, their general nature, and the fact that nonclassical properties of PADFS and PSDFS have not yet been accorded sufficient attention, has motivated us to perform this study.

Motivated by the above facts, in what follows, we investigate the possibilities of observing lower- and higher-order sub-Poissonian photon statistics, antibunching and squeezing in PADFS and PSDFS. We have studied nonclassical properties of these states through a set of other witnesses of nonclassicality, e.g., zeros of Q function, Mandel Q_M parameter, Klyshko's criterion, and Agarwal-Tara's criterion. These witnesses of nonclassicality successfully establish that both PADFS and PSDFS (along with most of the states to which these two states reduce at different limits) are highly nonclassical. Thus, making use of the analytical expressions of moments of creation and annihilation operators, discussed below, facilitates an analytical understanding for most of the nonclassical witnesses.

2.2 Higher-order moment for PADFS and PSDFS

We have already mentioned that we are interested in PADFS and PSDFS. In what follows, we will see that various experimentally measurable nonclassicality witnesses can be expressed as the moments of annihilation and creation operators Allevi et al. [2012b,a]; Avenhaus et al. [2010]; Peřina Jr et al. [2017]; Miranowicz et al. [2010]. To utilize those witnesses to identify the signatures of nonclassicality, we will compute an analytic expression for the most general moment, $\langle \hat{a}^{\dagger q} \hat{a}^r \rangle$, with q and r being non-negative integers. This is the most general moment in the sense that any other moment can be obtained as a special case of it. For example, if we need $\langle \hat{a}^2 \rangle$, we would just require to consider $q = 2$ and $r = 0$. Thus, an analytic expression for $\langle \hat{a}^{\dagger q} \hat{a}^r \rangle$ would essentially help us to obtain analytic expression for any moment-based witness of nonclassicality. Further, the analytic expressions of moment obtained for PADFS and PASDFS would also help us to obtain nonclassical features in the set of states obtained in the limiting cases, like Fock state, DFS, photon added coherent state. Keeping this in mind, we have computed $\langle \psi_+(u,n,\alpha)|\hat{a}^{\dagger q}\hat{a}^r|\psi_+(u,n,\alpha)\rangle$ and $\langle \psi_-(v,n,\alpha)|\hat{a}^{\dagger q}\hat{a}^r|\psi_-(v,n,\alpha)\rangle$ using Eq. (1.19) and (1.20), and provide the final analytic expressions of these moments without going into the mathematical details to maintain the flow of the chapter.

The obtained expressions for the above mentioned moments for PADFS and PSDFS are

$$\begin{aligned}\langle \hat{a}^{\dagger q}\hat{a}^{r}\rangle_{\text{PADFS}} &= \langle \psi_{+}(u,n,\alpha)|\hat{a}^{\dagger q}\hat{a}^{r}|\psi_{+}(u,n,\alpha)\rangle \\ &= \frac{N_{+}^{2}}{n!}\sum_{p,p'=0}^{n}\binom{n}{p}\binom{n}{p'}(-\alpha^{\star})^{(n-p)}(-\alpha)^{(n-p')} \\ &\times \exp\left[-\mid\alpha\mid^{2}\right]\sum_{m=0}^{\infty}\frac{\alpha^{m}(\alpha^{\star})^{m+p-p'-r+q}(m+p+u)!(m+p+u-r+q)!}{m!(m+p-p'-r+q)!(m+p+u-r)!},\end{aligned} \tag{2.1}$$

and

$$\begin{aligned}\langle \hat{a}^{\dagger q}\hat{a}^{r}\rangle_{\text{PSDFS}} &= \langle \psi_{-}(v,n,\alpha)|\hat{a}^{\dagger q}\hat{a}^{r}|\psi_{-}(v,n,\alpha)\rangle \\ &= \frac{N_{-}^{2}}{n!}\sum_{p,p'=0}^{n}\binom{n}{p}\binom{n}{p'}(-\alpha^{\star})^{(n-p)}(-\alpha)^{(n-p')} \\ &\times \exp\left[-\mid\alpha\mid^{2}\right]\sum_{m=0}^{\infty}\frac{\alpha^{m}(\alpha^{*})^{m+p-p'-r+q}(m+p)!(m+p-r+q)!}{m!(m+p-p'-r+q)!(m+p-v-r)!},\end{aligned} \tag{2.2}$$

respectively. The values of normalization constants for PADFS and PSDFS are already given in Eqs. (1.21) and (1.22), respectively. In the following section, we shall investigate the possibilities of observing various types lower- and higher-order nonclassical features in PADFS and PSDFS by using Eqs. (2.1) and (2.2).

2.3 Nonclassical features of PADFS and PSDFS

The moments of number operators for PADFS and PSDFS states obtained in the previous section enable us to study nonclassical properties of these states using a set of moments-based criteria of nonclassicality Miranowicz et al. [2010]Naikoo et al. [2018]. In the recent past, an infinite set of these moments-based criteria is shown to be equivalent to the P-function-based criterion, i.e., it becomes both necessary and sufficient Richter and Vogel [2002]; Shchukin and Vogel [2005b]. However, in this section, we will use a subset of this infinite set as witnesses of nonclassicality to investigate various nonclassical properties of the PADFS and PSDFS. Specifically, nonclassicality will be witnessed through Mandel Q_M parameter, criteria of lower- and higher-order antibunching, Agarwal-Tara's criterion, Klyshko's criterion, criteria of higher-order sub-Poissonian photon statistics, zeros of Q function, etc. As all these criteria are already introduced in Section 2.3, here we may discuss the plots and results.

2.3.1 Mandel Q_M Parameter

Negativity of this parameter indicates nonclassicality which can be calculated using Eqs. (2.1) and (2.2). In Figure 2.2, the dependence of Q_M on the state parameter α and non-Gaussianity inducing parameters (i.e., photon addition, subtraction, and Fock parameters as they can induce non-Gaussianity in a quantum state) is shown. Specifically, variation of Q_M parameter for PADFS and PSDFS is shown with state parameter α, where the effect of the number of photons added/subtracted and the initial Fock state is also established. For $\alpha = 0$, the PADFS with an arbitrary number of photon addition has Q_M parameter -1, which can be attributed to the fact that final state, which

reduces to the Fock state ($|1\rangle$ chosen to be displaced in this case) is the most nonclassical state (cf. Figure 2.2 (a)). With increase in the number of photons added to the DFS, the depth of nonclassicality witness Q_M increases. However, the witness of nonclassicality becomes less negative for higher values of the displacement parameter. In contrast to the photon addition, with the subtraction of photons from the DFS the Q_M parameter becomes almost zero for the smaller values of displacement parameter α in DFS as shown in Figure 2.2 (c). This behavior can be attributed to the fact that photon subtraction from $D(\alpha)|1\rangle$ for small values of α will most likely yield vacuum state. Also, with the increase in the displacement parameter the witness of nonclassicality becomes more negative as with a higher average number of photons in DFS photon subtraction becomes more effective. However, for the larger values of displacement parameter the nonclassicality disappears analogous to the PADFS. For large values of α, this parameter dominates in the behavior of the state and thus it behaves analogous to coherent state.

As Fock states are known to be nonclassical, and photon addition and subtraction are established as nonclassicality inducing operations, it would be worth comparing the effect of these two independent factors responsible for the observed nonclassical features in the present case. To perform this study, we have shown the variation of the single photon added (subtracted) DFS with different initial Fock states in Figure 2.2 (b) (Figure 2.2 (d)). Specifically, the nonclassicality present in PADFS decays faster for the higher values of the Fock states with increasing displacement parameter (cf. Figure 2.2 (b)). However, such nature was not present in PSDFS shown in Figure 2.2 (d). Note that variation of Q_M parameter with α starts from 0 (-1) iff $u \leq n$ ($u > n$). For instance, if $u = n = 1$, i.e., corresponding to state $\hat{a}D(\alpha)|1\rangle$, nonclassicality witness is zero for $\alpha = 0$ as it corresponds to vacuum state. Therefore, the present study reveals that photon addition is a stronger factor for the nonclassicality present in the state when compared to the initial Fock state chosen to be displaced. Whereas photon subtraction is a preferred choice for large values of displacement parameter in contrast to the higher values of Fock states to displace with small α. Among photon addition and subtraction, addition is a preferred choice for the smaller values of displacement parameter, while the choice between addition and subtraction becomes immaterial for large α.

2.3.2 Lower- and higher-order antibunching

The nonclassicality reflected by the lower-order antibunching criterion obtained here is the same as Mandel Q_M parameter $\left(Q_M = \frac{d(1)}{\langle \hat{a}^\dagger \hat{a} \rangle}\right)$ illustrated in Figure 2.2. Therefore we will rather discuss here the possibility of observing higher-order antibunching in the quantum state of our interest using Eqs. (2.1) and (2.2) in Eq. (1.41). Specifically, the depth of nonclassicality witness can be observed to increase with order for both PADFS and PSDFS as depicted in Figure 2.3 (a) and (d). This fact is consistent with the earlier observations (Thapliyal et al. [2014a,b, 2017b,a]; Alam et al. [2017b] and references therein) that higher-order nonclassicality criteria are useful in detecting weaker nonclassicality. On top of that the higher-order antibunching can be observed for larger values of displacement parameter α, when lower-order antibunching is not present. The presence of higher-order nonclassicality in the absence of its lower-order counterpart establishes the relevance of the present study.

The depth of nonclassicality parameter ($d(l-1)$) was observed to decrease with an increase in the number of photons subtracted from DFS for small values of α in Figure 2.2 (c). A similar nature is observed in Figure 2.3 (e), which shows that for the higher values of displacement parameter, the depth of higher-order nonclassicality witness increases with the number of photon

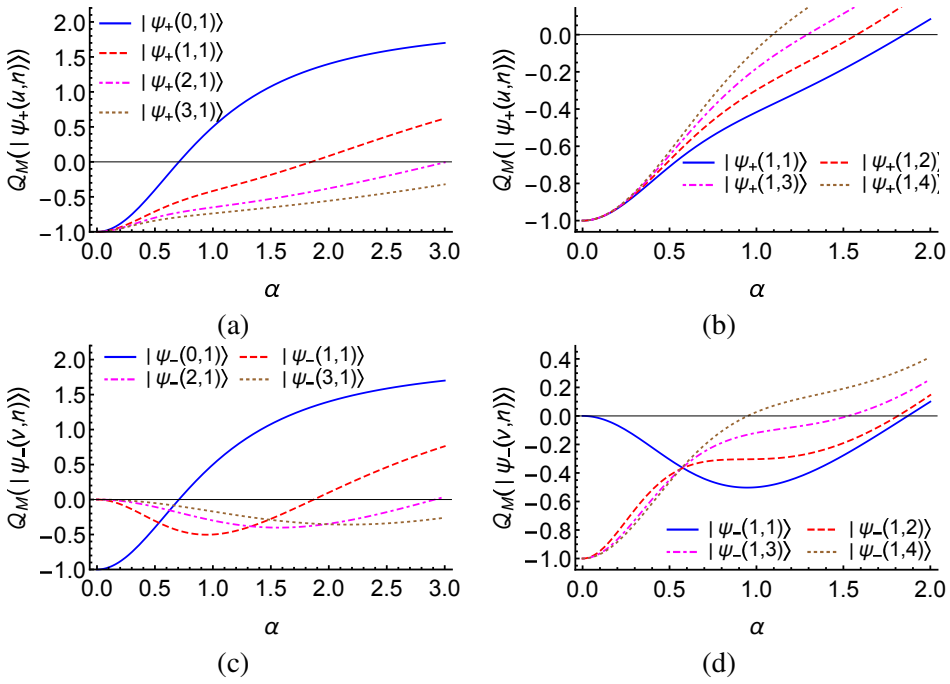

Figure 2.2: Variation of Mandel Q_M parameter for PADFS (in (a) and (b)) and PSDFS (in (c) and (d)) is shown with displacement parameter α. In (a) and (c), the value of number of photons added/subtracted (i.e., u or v) is changed for the same initial Fock state $|1\rangle$. Different initial Fock states $|n\rangle$ are chosen to be displaced in (b) and (d) for the single photon addition/subtraction. The blue curve corresponds to vacuum for $\alpha = 0$ and thus starts from 0 unlike rest of the states which are Fock state ($n \neq 0$) in the limiting case. Therefore, nonclassicality increases first with increasing α before decreasing as in the rest of the cases.

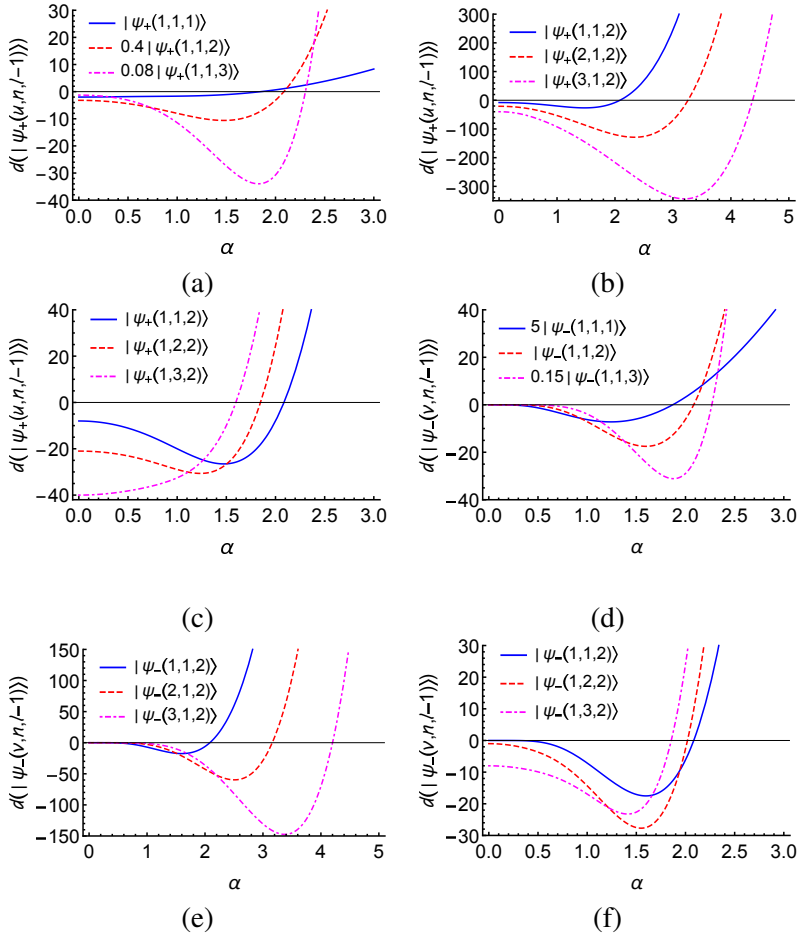

Figure 2.3: The presence of higher-order antibunching is shown as a function of α for PADFS (in (a)-(c)) and PADFS ((d)-(f)). Specifically, (a) and (d) illustrate comparison between lower- and higher-order antibunching. It should be noted that some of the curves are multiplied by a scaling factor in order to present them in one figure. Figures (b) and (e) show the effect of photon addition/subtraction, and (c) and (f) establish the effect of Fock state chosen to displace in PADFS and PSDFS, respectively. Here, without the loss of generality, we have used the notation $\psi_+(u,n,l-1)$ ($\psi_-(u,v,l-1)$) for nonclassicality in photon added (subtracted) scenarios, and will follow this notation in subsequent figures of this chapter.

subtraction. Therefore, not only the depth of nonclassicality but the range of displacement parameter for the presence of higher-order antibunching also increases with photon addition/subtraction (cf. Figure 2.3 (b) and (e)). With the increase in the value of Fock state parameter n, the depth of higher-order nonclassicality witness increases (decreases) for smaller (larger) values of displacement parameter in both PADFS and PSDFS as shown in Figure 2.3 (c) and (f), respectively. Thus, we have observed that the range of α with the presence of nonclassicality increases (decreases) with photon addition/subtraction (Fock state) in DFS.

2.3.3 Higher-order sub-Poissonian photon statistics

This allows us to study higher-order sub-Poissonian photon statistics using Eqs. (2.1) and (2.2) in Eq. (1.42). The presence of higher-order sub-Poissonian photon statistics (as can be seen in Figure 2.4 (a) and (d) for PADFS and PSDFS, respectively) is dependent on the order of nonclassical-

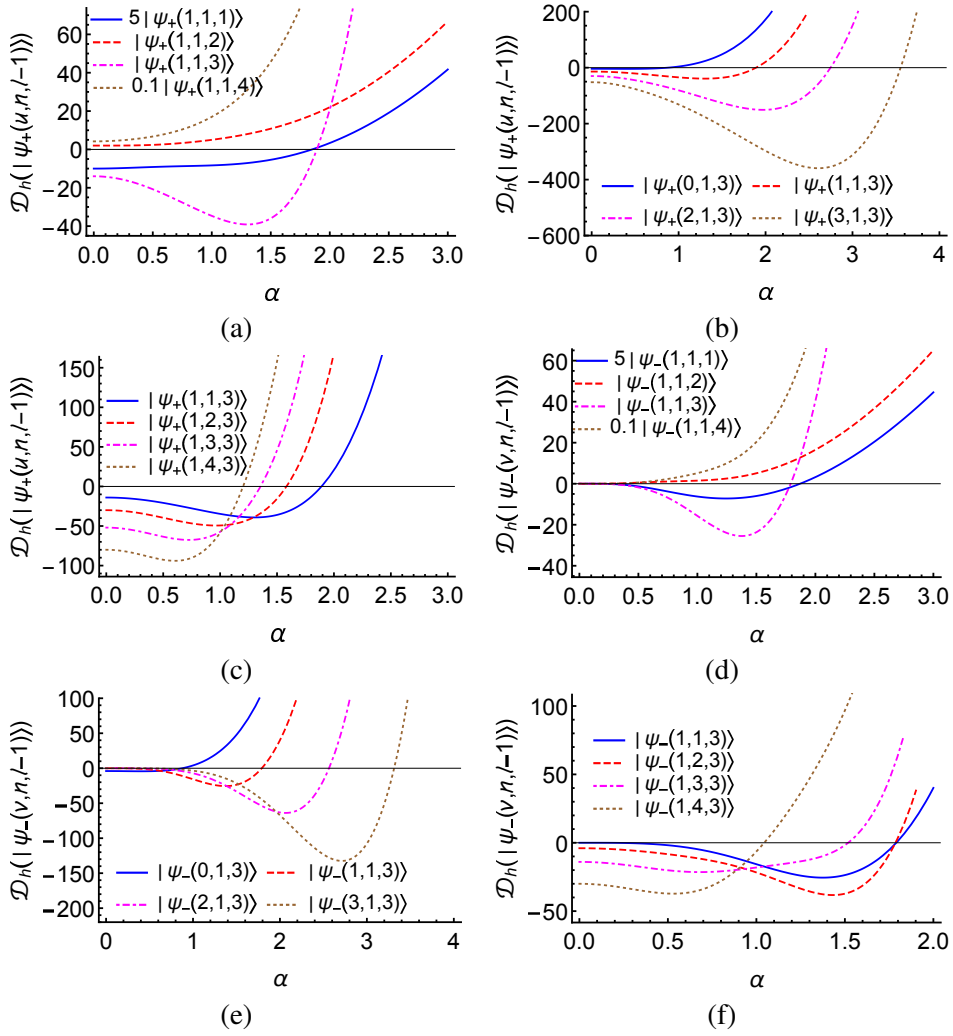

Figure 2.4: Dependence of higher-order sub-Poissonian photon statistics on α for PADFS (in (a)-(c)) and PSDFS ((d)-(f)) is illustrated here. Specifically, (a) and (d) show the increase in depth of nonclassicality witness with order, (b) and (e) depict the effect of photon addition and subtraction, respectively, and (c) and (f) establish the effect of choice of Fock state to be displaced in PADFS and PSDFS, respectively.

ity unlike higher-order antibunching, which is observed for all orders. Specifically, the nonclassical feature was observed only for odd orders, which is consistent with some of the earlier observations Thapliyal et al. [2017b], where nonclassicality in those cases could be induced due to squeezing. Along the same line, we expect to observe the nonclassicality in such cases with appropriate use of squeezing as a useful quantum resource, which will be discussed elsewhere. In case of photon addition/subtraction in DFS, a behavior analogous to that observed for higher-order antibunching is observed, i.e., the depth of nonclassciality increases with the photon addition while it decreases (increases) for small (large) values of α (cf. Figure 2.4 (b) and (e)). Similar to the previous case, nonclassicality can be observed to be present for larger values of displacement parameter with photon addition/subtraction, while increase in the value of Fock parameter has an opposite effect.

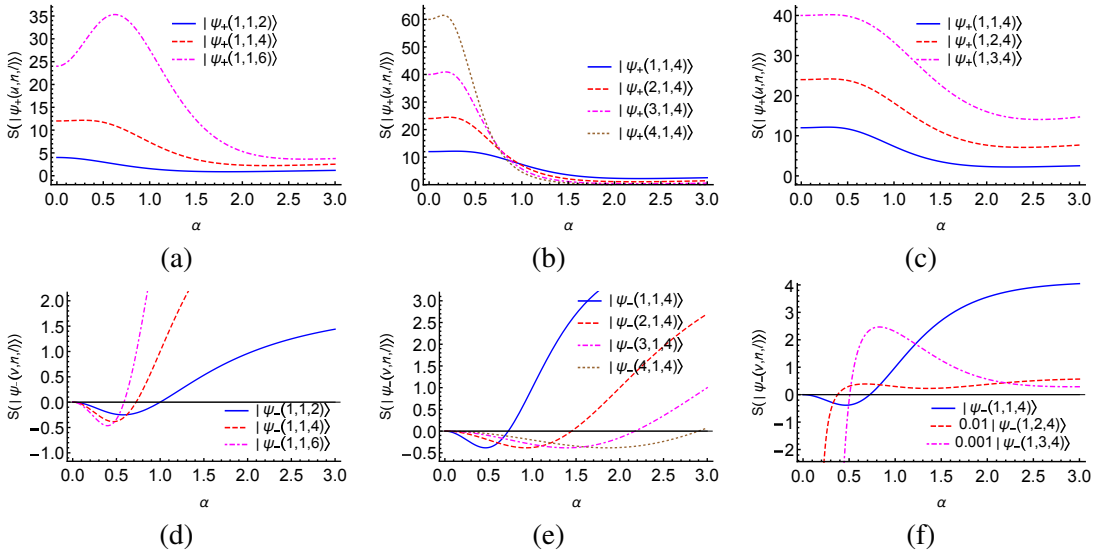

Figure 2.5: Illustration of the higher-order squeezing using Hong-Mandel criterion as the function of displacement parameter. In (a) and (d), dependence of the observed nonclassicality on different orders (l) is shown for PADFS and PSDFS, respectively; while in (b) and (e), the effect of variation in the number of photon added/subtracted is shown in case of PADFS and PSDFS, respectively. In (c) and (f), the variation due to change in the initial Fock state chosen to be displaced is shown for PADFS and PSDFS, respectively.

2.3.4 Higher-order squeezing

The analytical expressions of the nonclassicality witness of the Hong-Mandel type higher-order squeezing criterion for PADFS and PSDFS can be obtained with the help of Eqs. (2.1), (2.2), and (1.43)-(1.45). We have investigated the higher-order squeezing and depict the result in Figure 2.5 assuming α to be real. Incidentally, we could not establish the presence of higher-order squeezing phenomena in PADFS (Figure 2.5 (a)-(c)). However, the depth of the higher-order squeezing witness increases with order for small values of α as shown in Figure 2.5 (a), while for the higher values of the displacement parameter, higher-order squeezing disappear much quicker (cf. Figure 2.5 (d)). With increase in the number of photons subtracted, the presence of this nonclassicality feature can be maintained for the higher values of displacement parameter as well (cf. Figure 2.5 (e)). In general, photon subtraction is a preferred mode for nonclassicality enhancement as far as this non-classciality feature is concerned. The choice of the initial Fock state is also observed to be relevant as the depth of squeezing parameter can be seen increasing with value of the Fock parameter for PSDFS in the small displacement parameter region (shown in Figure 2.5 (f)), where this nonclassical behavior is also shown to succumb to the higher values of Fock and displacement parameters. Unlike the other nonclassicalities discussed so far, the observed squeezing also depends on phase θ of the displacement parameter $\alpha = |\alpha|\exp(i\theta)$ due to the second last term in Eq. (1.45). We failed to observe this nonclassicality behavior in PADFS even by controlling the value of the phase parameter (also shown in Figure 2.6 (a)). For PSDFS, the squeezing disappears for some particular values of the phase parameter, while the observed squeezing is maximum for $\theta = n\pi$ (see Figure 2.6 (b)). It thus establishes the phase parameter of the displacement operator as one more controlling factor for nonclassicality in these engineered quantum states.

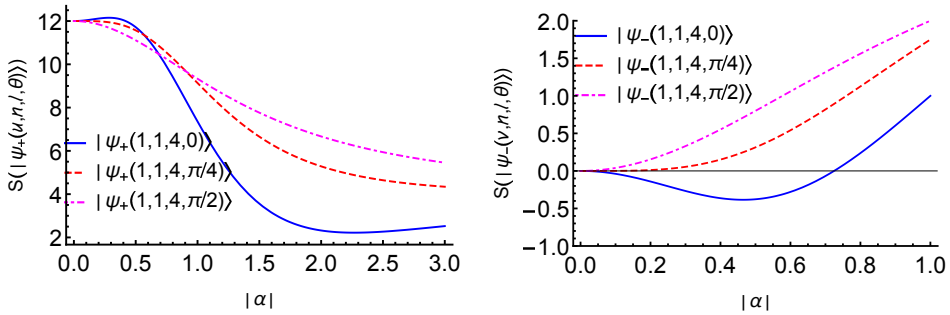

(a) (b)

Figure 2.6: Hong-Mandel type higher-order squeezing for PADFS and PSDFS is shown dependent on the phase of the displacement parameter $\alpha = |\alpha| \exp(i\theta)$ in (a) and (b), respectively.

2.3.5 Q function

Using Eqs. (1.19) and (1.20) in (1.50), we obtain the analytic expressions for the Husimi Q function for PADFS and PSDFS as

$$\begin{aligned} Q_+ &= \frac{N_+^2}{\pi}\frac{\exp\left[-|\beta|^2\right]}{n!}\sum_{p,p'=0}^{n}\binom{n}{p}\binom{n}{p'}(-\alpha^\star)^{(n-p)}(-\alpha)^{(n-p')}\exp\left[-|\alpha|^2\right] \\ &\times \sum_{m,m'=0}^{\infty}\frac{\alpha^m(\alpha^\star)^{m'}\beta^{(m'+p'+u)}(\beta^\star)^{(m+p+u)}}{m!m'!} \end{aligned} \tag{2.3}$$

and

$$\begin{aligned} Q_- &= \frac{N_-^2}{\pi}\frac{\exp\left[-|\beta|^2\right]}{n!}\sum_{p,p'=0}^{n}\binom{n}{p}\binom{n}{p'}(-\alpha^\star)^{(n-p)}(-\alpha)^{(n-p')}\exp\left[-|\alpha|^2\right] \\ &\times \sum_{m,m'=0}^{\infty}\frac{\alpha^m(\alpha^\star)^{m'}\beta^{(m'+p'-v)}(\beta^\star)^{(m+p-v)}(m+p)!(m'+p')!}{m!m'!(m+p-v)!(m'+p'-v)!}, \end{aligned} \tag{2.4}$$

respectively. We failed to observe the nonclassical features reflected beyond moments based nonclassicality criteria through a quasiprobability distribution, i.e., zeros of the Q function. We have shown the Q function in Figure 2.7, where the effect of photon addition/subtraction and the value of Fock parameter on the phase space distribution is shown. Specifically, it is observed that the value of Fock parameter affects the quasidistribution function more compared to the photon addition/subtraction.

2.3.6 Agarwal-Tara's criterion

The analytic expression of A_3 parameter defined in Eq. (1.48) can be obtained for PADFS and PSDFS using Eqs. (2.1) and (2.2). The nonclassical properties of the PADFS and PSDFS using Agarwal-Tara's criterion are investigated, and the corresponding results are depicted in Figure 2.8, which shows highly nonclassical behavior of the states generated by engineering. Specifically, the negative part of the curves, which is bounded by -1, ensures the existence of the nonclassicality. From Figure 2.8, it is clear that A_3 is 0 (-1) for the displacement parameter $\alpha = 0$ because then DFS, PADFS, and PSDFS reduce to Fock state, and $A_3 = 0$ (-1) for the Fock state parameter $n = 0, 1$ $(n > 1)$. Nonclassicality reflected through A_3 parameter increases (decreases) with photon addition (subtraction) (shown in Figure 2.8 (a) and (c)). In contrast, the Fock parameter has a completely op-

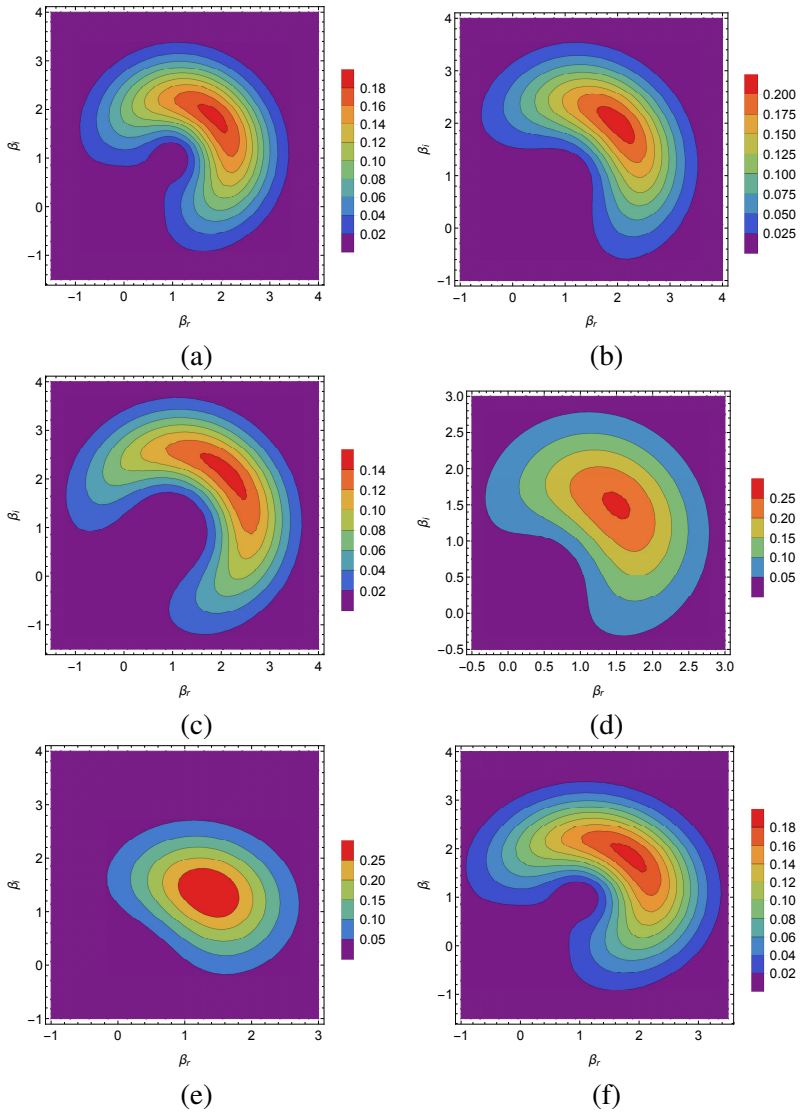

Figure 2.7: Contour plots of the Q function for (a) single photon added displaced Fock $|1\rangle$ state, (b) two photon added displaced Fock $|1\rangle$ state, (c) single photon added displaced Fock $|2\rangle$ state, (d) single photon subtracted displaced Fock $|1\rangle$ state, (e) two photon subtracted subtracted displaced Fock $|1\rangle$ state, (f) single photon subtracted displaced Fock $|2\rangle$ state. In all cases, $\alpha = \sqrt{2}\exp\left(\frac{i\pi}{4}\right)$ is chosen.

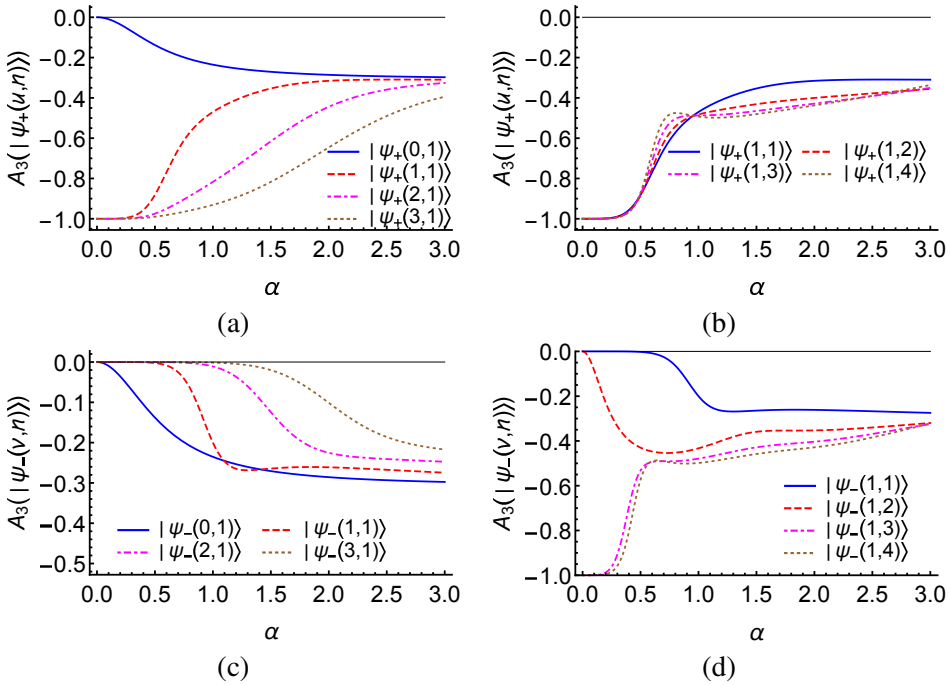

Figure 2.8: Variation of Agarwal-Tara's parameter with α for PADFS and PSDFS is shown in (a)-(b) and (c)-(d), respectively. Specifically, the effect of photon addition/subtraction (in (a) and (c)) and the choice of Fock state ((b) and (d)) on the presence of nonclassicality in PADFS and PSDFS is illustrated.

posite effect that it leads to decrease (increase) in the observed nonclassicality for PADFS (PSDFS), which can be seen in Figure 2.8 (b) and (d). However, for larger values of displacement parameter, the depth of nonclassicality illustrated through this parameter can again be seen to increase (cf. Figure 2.8 (b)).

2.3.7 Klyshko's Criterion

The analytic expression for the mth photon-number distribution for PADFS and PSDFS can be calculated (using $q = r = 1$) from Eqs. (2.1) and (2.2), respectively.

The advantage of the Klyshko's criterion over any other existing moments based criteria is that a very small amount of information is required. Specifically, probability of only three successive photon numbers is sufficient to investigate the nonclassical property. The negative values of $B(m)$ serve as the witness of nonclassicality. Klyshko's criterion in Eq. (1.46) is derived analytically and the corresponding nonclassical properties for both PADFS and PSDFS are investigated (cf. Figure 2.9). Specifically, the negative values of $B(m)$ are observed for different values of m in case of photon addition and subtraction (cf. Figure 2.9 (a) and (c)) being the signature of nonclassicality induced via independent operations. Additionally, one can also visualize that due to the photon addition (subtraction) the negative peaks in the values of $B(m)$ shift to higher (lower) photon number regime. A similar observation is obtained for different values of the Fock state parameter for the PADFS and PSDFS, where the negative values of the witness of nonclassicality get amplified towards higher photon number regime and becomes more negative, and the corresponding results are shown in Figure 2.9 (b) and (d), respectively. This further establishes the relevance of operations, like photon addition, subtraction, and starting with Fock states in inducing nonclassicality in the engineered

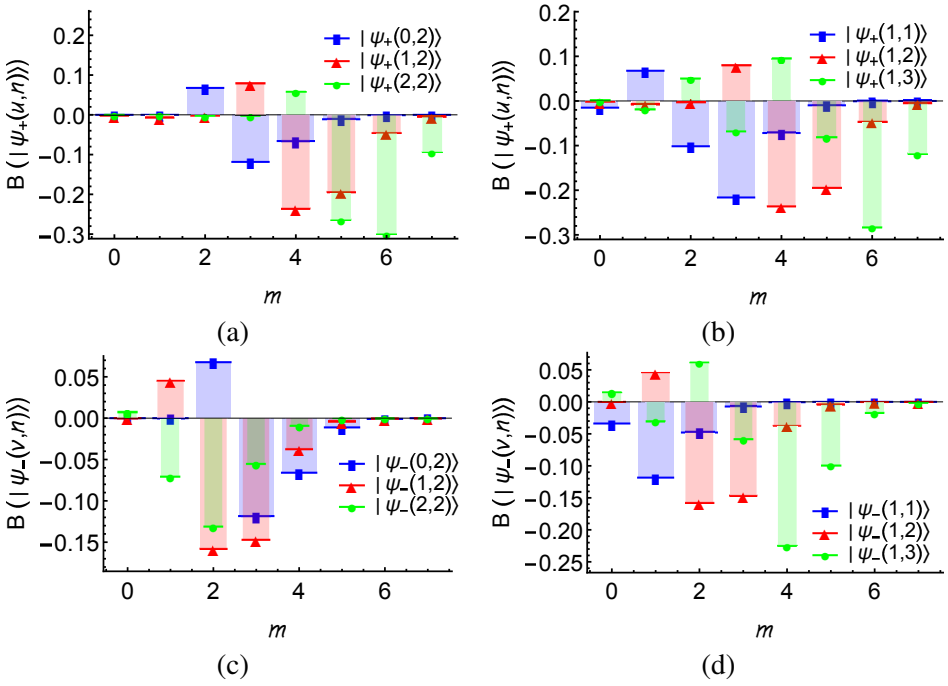

Figure 2.9: Illustration of the Klyshko's criterion. Variation of $B(m)$ with respect to m (a) and (c) for different values of the number of the photon additon/subtraction for PADFS and PSDFS, respectively; (b) and (d) for different values of the number of the Fock state parameter for PADFS and PSDFS, respectively. Here, we have chosen $\alpha = 1$ in all cases because almost all of the other criteria detected nonclassicality for this choice of α so does the Klyshko's criterion.

quantum states.

2.4 Conclusions

The only Fock state that does not show any nonclassical feature is the vacuum state Miranowicz et al. [2015], and displacement operator preserves its classicality. All the rest of the Fock states are maximally nonclassical and they are shown to remain nonclassical even after application of a displacement operator. Here, we set ourselves a task: What happens when the displacement operator applied on a Fock state is followed by addition or subtraction of photon(s)? Independently, photon addition and subtraction are already established as nonclassicality inducing operations in case of displaced vacuum state (i.e., coherent state). In this chapter, we have established that photon addition/subtraction is not only nonclassicality inducing operation, it can also enhance the nonclassicality present in the DFS. It's expected that these operations would increase the amount of nonclassicality (more precisely, the depth of the nonclassicality witnessing parameter) present in other nonclassical states, too. There is one more advantage of studying the nonclassical features of PADFS and PSDFS. These states can be reduced to a class of quantum states, most of which are already experimentally realized and found useful in several applications. Inspired by the available experimental results, we have also proposed optical designs for generation of PADFS and PSDFS from the squeezed vacuum state.

To analyze the nonclassical features of the engineered final states, i.e., PADFS and PS-

DFS, we have used a set of moments based criteria, namely Mandel Q_M parameter, Agarwal-Tara's A_3 parameter, criteria for higher-order antibunching, sub-Poissonian photon statistics, and squeezing. In addition, the nonclassical features have been investigated through Klyshko's criterion and a quasiprobability distribution–Q function. The states of interest are found to show a large variety of nonclassical features as all the nonclassicality witnesses used here (except Q function) are found to detect the nonclassicality. They show that state is useful as squeezed, antibunched, as well as generation of entangled state.

This study has revealed that the amount of nonclassicality in PADFS and PSDFS can be controlled by the Fock state parameter, displacement parameter, the number of photons added or subtracted. In general, the amount of nonclassicality with respect to the witness used here is found to increase with the number of photons added/subtracted, while smaller values of Fock state and displacement parameters are observed to be preferable for the presence of various nonclassical features. On some occasions, nonclassicality has also been observed to increase with the Fock state parameter, while larger values of displacement parameter always affect the nonclassicality adversely. Most of the nonclassicality criteria used here, being moments-based criteria, could not demonstrate the effect of phase parameter of the displacement parameter. Here, higher-order squeezing witness and Q function are found to be dependent on the phase of the displacement parameter. However, only higher-order squeezing criterion was able to detect nonclassicality, and thus established that this phase parameter can also be used to control the amount of nonclassicality.

Further, in the past, it has been established that higher-order nonclassicality criteria have an advantage in detecting weaker nonclassicality. We have also shown that the depth of nonclassicality witness increases with order of nonclassicality thus providing an advantage in the experimental characterization of the observed nonclassical behavior.